PHILOSOPHICAL TRANSACTIONS OF THE ROYAL SOCIETY A
MATHEMATICAL, PHYSICAL & ENGINEERING SCIENCES

Trace Element Fractionation Processes in the Generation of Island Arc Basalts

C. J. Hawkesworth, K. Gallagher, J. M. Hergt and F. Mc Dermott

Phil. Trans. R. Soc. Lond. A 1993 **342**, 179-191
doi: 10.1098/rsta.1993.0013

Trace element fractionation processes in the generation of island arc basalts

By C. J. Hawkesworth, K. Gallagher, J. M. Hergt† and F. McDermott
Department of Earth Sciences, The Open University, Milton Keynes MK7 6AA, U.K.

Subduction-related magmas are characterized by distinctive minor and trace element ratios which are widely attributed to the introduction of a hydrous component from the subducted crust. Island arc rocks may usefully be subdivided into high and low Ce/Yb groups, and the latter are characterized by relatively restricted radiogenic isotope ratios. In general, high LIL/HFSE ratios are best developed in low HFSE rocks, and the variation in LILE is less than that in HFSE. A local equilibrium model is developed in which the distinctive minor and trace element feature of arc rocks are the result of fluid percolation in the mantle wedge. Peridotite/fluid distribution coefficients are inferred to vary systematically with ionic radius in the range $69–167 \times 10^{-12}$ m. However, in practice the calculated olivine/fluid partition coefficients are too high to develop an arc signature in the wedge peridotite in reasonable timescales, and for acceptable fluxes from the slab. The available geochemical data would suggest that realistic distribution coefficients are 2–3 orders of magnitude less than those presently available from experimental data, presumably because the fluid compositions are different, or that local equilibrium is not appropriate. Average compositions from the low Ce/Yb arc suites exhibit a positive correlation between Ce/Sm, but not K/Sm, and crustal thickness. It is argued that the degree of melting varies with crustal thickness, but not in any simple way with the magnitude of the fluid contribution. The observed range in Ce/Sm in the low Ce/Yb rocks is consistent with 3–18% melting of slightly LREE depleted source rocks.

1. Introduction

Magma generation along destructive plate margins differs significantly from that in other tectonic settings. First, subduction-related magmas have distinctive minor and trace element compositions; second, considerable volumes of magma are generated despite the depression of mantle isotherms caused by the subduction of cold oceanic crust; and third, partial melting appears to be initiated by the introduction of water and depression of the peridotite solidus, rather than by diapiric upwelling and decompression. Recent studies have reviewed the major element variations in arc magmas, and sought to model them in the light of the limited experimental data available (Plank & Langmuir 1988; Davies & Bickle 1991). This contribution therefore discusses some of the minor and trace element features of magmas generated above subduction zones, and evaluates the extent to which they are consistent with the major element models.

---

† Present address: Research School of Earth Sciences, The Australian National University, GPO Box 4, Canberra, ACT 2601, Australia.

Phil. Trans. R. Soc. Lond. A (1993) **342**, 179–191
Printed in Great Britain

Plank & Langmuir (1988) concluded that both the major element abundances, and the inferred degrees of melting, for primitive mid-ocean ridge (MOR) and arc basalts were surprisingly similar. Whatever the causes of melting in the two environments, this conclusion was taken as further evidence that in most cases it is the mantle wedge which melts beneath arcs, rather than the subducted slab. In detail, Plank & Langmuir (1988) re-emphasized the near constancy of the depth to the Benioff Zone beneath volcanic arcs, at *ca.* 110 km, which suggests that arc magmatism is linked to a pressure sensitive reaction, such as the breakdown of amphibole. They also demonstrated that Na_2O at 6% MgO increased, and CaO at 6% MgO decreased significantly with increasing thickness of the arc crust. Variations of other chemical features, such as average SiO_2, with crustal thickness have been described previously (Coulon & Thorpe 1981; Leeman 1983), but for the most part attributed to increased fractional crystallization and crustal contamination in areas of thicker crust. However, the variations in Na_2O and CaO at 6% MgO are difficult to explain by any such shallow level processes, rather they are consistent with a model in which the average degree of melting depends on the thickness of the melting column (Plank & Langmuir 1988).

2. Minor and trace elements, and radiogenic isotopes

Several minor and trace element features of subduction-related rocks are consistently different from those of MORB and OIB, and in particular they are characterized by high LIL/HFS element ratios, and relatively low Nb, Ta, and perhaps Ti abundances (Pearce 1982). In contrast, the majority of destructive plate margin rocks have Nd, Sr and Pb isotope ratios which are broadly similar to those of OIB (Morris & Hart 1983; Hawkesworth *et al.* 1991*a*), and to those of MORB which have more enriched isotope signatures (higher $^{87}Sr/^{86}Sr$ and lower $^{143}Nd/^{144}Nd$). Some subduction related rocks exhibit steep arrays on Pb isotope diagrams (Kay *et al.* 1978; Woodhead & Fraser 1985; White & Dupré 1986), consistent with the introduction of radiogenic Pb from subducted sediments, and more recently it has been demonstrated that young arc rocks often exhibit high ^{10}Be which requires a contribution from young (less than 5 Ma) sedimentary material, presumably in the subducted slab (Tera *et al.* 1986; Morris *et al* 1990). In general, however, the isotope data on subduction-related rocks suggest that the contributions from sediments and altered oceanic crust in the subducted slab are typically much less than estimates of the 'subduction component' calculated on the basis of minor and trace element variations (Pearce 1983; Hawkesworth *et al.* 1991*a*).

The rare earth elements (REE) are widely used in models of petrogenesis, both because they are a geochemically coherent group and because they include the radioactive decay scheme of ^{147}Sm to ^{143}Nd. A key step is to identify rock suites which may have been derived from similar source regions, and Hawkesworth *et al.* (1991*a*) pointed out that the REE results from destructive plate margin rocks broadly fall into two groups. In one, Ce and Yb vary together, and in the other the Ce contents are much higher and the Yb contents are similar. Such differences require major differences in either the REE profiles of the source rocks for the two groups, and/or in the bulk distribution coefficients and the degree of melting. Rocks in the high Ce/Yb group have a much greater range in Nd, Sr and Pb isotope ratios, and so the simplest interpretation is that they contain at least a contribution from material which in many cases was both old (i.e. old enough to have developed

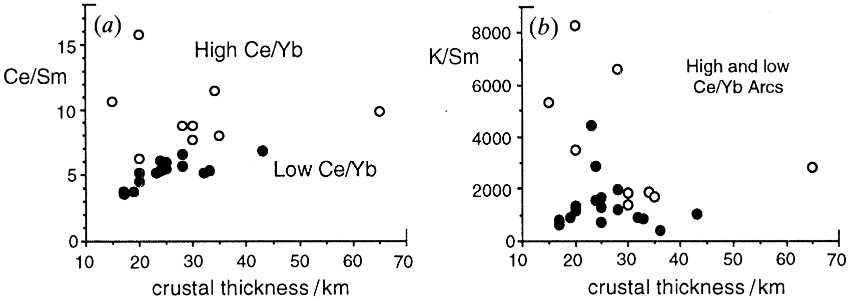

Figure 1. Variations in the average Ce/Sm and K/Sm ratios of arc rocks with crustal thickness. The low Ce/Yb arcs (●) include data from the Aleutians, Andes (SVZ), Central Americas, Fiji, Halmahera, Honshu, Kermadecs, Kuriles, L. Antilles, Papua, Marianas, NE Sulawesi, New Britain, Tonga and Vanuatu: the high Ce/Yb arcs (○) include data from the Aeolian Islands, Andes (CVZ), Costa Rica, Grenada, Java, Papua, Muriah, the Philippines and Sunda (references in Hawkesworth *et al.* 1991*b*). Average MgO contents = 4.9–7.8%, and there is no systematic variation between Ce/Sm and MgO.

different isotope ratios), and LREE enriched. Such features have been attributed both to subducted sediments and to trace element enriched source regions in the mantle wedge.

The dilemma facing any analysis of partial melting processes from minor and trace element data is the minor and trace element composition of the source, and whether that can be inferred from chemical trends in the more primitive rock samples, or it must be assumed. McKenzie & O'Nions (1991) used inverse theory to calculate the melt fractions with depth required to produce the REE concentrations in magmatic rocks from different tectonic settings. They chose to average selected data-sets, and to assume the REE contents of the magma source regions. Such calculations reaffirm the sensitivity of REE profiles to the presence or absence of residual garnet, and they encouraged McKenzie & O'Nions to invoke residual amphibole in the source of island arc magmas. However, they also indicate that for ratios of LREE, such as Ce/Sm, the rate of change with degree of melting is similar for garnet-free and garnet-bearing assemblages. Consequently Ce/Sm ratios may be used crudely to evaluate differences in the average degree of melting irrespective of the proportion of melting that took place in the garnet and spinel stability fields.

To evaluate the extent to which REE and other trace element ratios vary with crustal thickness, as demonstrated for Na_2O and CaO at 6% MgO (Plank & Langmuir 1988), average values have been compiled for arc rocks with less than 53% SiO_2. Within the low Ce/Yb group of arcs, average Ce/Sm increases from 3.6 to 6.9 as the crustal thickness increases from *ca.* 18 km at Tonga and the Northern Lesser Antilles to *ca.* 43 km in the Southern Andes. Similarly there is a broad positive correlation between average Ce/Sm and Na_2O/CaO. However, the high Ce/Yb arcs show much more scatter, and many of them are predictably displaced to higher Ce/Sm for any particular crustal thickness (figure 1*a*). Since the high Ce/Yb suites tend to have lower $^{143}Nd/^{144}Nd$, their higher Ce/Sm ratios are inferred, at least in part, to reflect their different source compositions. However, the variation in Ce/Sm within the low Ce/Yb rocks is consistent with different degrees of partial melting, with the smaller degrees of partial melting occurring in areas of thicker crust.

Fractional crystallization can affect REE ratios even in rocks with less than 53% SiO_2, and so it might be argued that the increase in Ce/Sm with crustal thickness in figure 1 is a function of more fractional crystallization in areas of thicker crust. However, using the D values in table 1, 50% clinopyroxene fractionation only changes Ce/Sm in the residual magma by 10%. Amphibole also fractionates REE ratios, but in this case Sm/Yb decreases as Ce/Sm increases, whereas in the rocks studied here there is a positive correlation between Ce/Sm and Sm/Yb. Thus it would appear that the differences between the average Ce/Sm ratios have not been changed significantly by fractional crystallization processes. Rather, if it is simply assumed that the low Ce/Yb rocks were derived from source regions with similar REE ratios, the observed range in Ce/Sm can be generated by *ca.* 3–18% fractional melting of a slightly LREE depleted source, using the distribution coefficients in table 1.

The distinctive relatively high LILE contents of arc rocks can be illustrated by the variations in K/Sm and, in contrast to Ce/Sm, there is no systematic variation of K/Sm with crustal thickness (figure 1*b*). The simplest interpretation is that the variation in K/Sm does not primarily reflect partial melting processes. Minor and trace element variations in arc basalts indicate that if the high K/Sm and high LIL/HFSE ratios were due to partial melting processes, for example, then $D_{\mathrm{Sm}} \gg D_{\mathrm{K}}$ and $D_{\mathrm{Ce}} > D_{\mathrm{Nb}}$. Many authors have concluded that this is unlikely, and that the relatively high LILE contents of subduction-related rocks are instead due to scavenging by hydrous fluids, from the slab and/or the mantle wedge (Pearce 1982; Arculus & Powell 1986; Tatsumi *et al.* 1986).

3. Melt and fluid percolation

Beneath volcanic arcs, hydrous fluids from the subducted slab, and subsequently partial melts, must migrate through mantle which is being dragged down by convection. During this fluid movement, trace and minor elements may be fractionated because of their differing effective transport velocities relative to the solid matrix (McKenzie 1984; Navon & Stolper 1987; McKenzie & O'Nions 1991). In the one-dimensional problem, assuming instantaneous local equilibrium between the fluid and the matrix during percolation, the effective velocity for an element i is

$$U_{\mathrm{e}}^{i} = FU_{\mathrm{f}} \tag{1}$$

with $F = 1/(1+D^{i}/N)$ and U_{f} is the fluid velocity relative to a static matrix, N is the fluid/solid mass ratio and D^{i} is the solid/fluid partition coefficient. Thus, provided the initial fluid composition is different from that in equilibrium with the matrix, all minor and trace elements will move more slowly than the bulk fluid. In the absence of diffusion and dispersion, a constant flux of fluid of a given composition results in concentration fronts for individual elements. For the ith element, moving with velocity U_{e}^{i}, the fluid ahead of the front is in equilibrium with the pre-fluid element concentration in the matrix, while the fluid behind the front maintains its original composition, with the relative concentrations determined by the appropriate partition coefficient. In a subduction zone, where solid material in the wedge overlying the slab is moving down with velocity U_{s}, then, in steady state, a concentration front, C_{f}, lies along a direction given by (Navon & Stolper 1987)

$$(\partial z/\partial x)_{C_{\mathrm{f}}} = (FU_{\mathrm{f}} - U_{\mathrm{s}} \sin \alpha)/U_{\mathrm{s}} \cos \alpha, \tag{2}$$

where α is the dip of the subduction zone from the horizontal. Clearly, if $F < (U_{\mathrm{s}}/U_{\mathrm{f}}) \sin \alpha$ then $(\partial z/\partial x)_{C_{\mathrm{f}}} < 0$, and the concentration front for an element with such a value

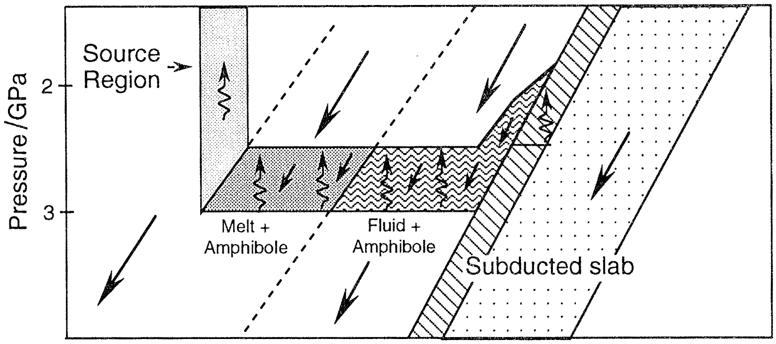

Figure 2. Schematic model for the release of hydrous fluids from the subducted slab and lateral migration to the zone of melt generation (after Davies & Bickle 1991). The fluids traverse laterally by a combination of vertical movement as a fluid, and downward movement fixed in amphibole carried down by induced mantle flow (straight arrows). In the preferred model, element fractionation may result from the percolation of first a hydrous fluid, and subsequently a partial melt through a peridotite matrix, and then during partial melting in the magma source regions.

Table 1. *Selected mineral/melt distribution coefficients used in this study*

	olivine	opx	cpx	spinel	garnet	amphibole
Pb	10^{-4}	1.3×10^{-3}	10^{-2}	5×10^{-4}	5×10^{-4}	10^{-1}
Rb	1.8×10^{-4}	6×10^{-4}	1.1×10^{-2}	5×10^{-4}	7×10^{-4}	2×10^{-1}
Ba	10^{-4}	6×10^{-4}	10^{-2}	5×10^{-4}	7×10^{-4}	2.5×10^{-1}
K	10^{-4}	6×10^{-4}	10^{-2}	5×10^{-4}	7×10^{-4}	8×10^{-1}
Th	1.1×10^{-4}	10^{-4}	2.6×10^{-4}	10^{-3}	10^{-4}	7×10^{-2}
U	10^{-4}	10^{-4}	3.6×10^{-4}	10^{-3}	10^{-4}	9×10^{-2}
Nb	10^{-2}	10^{-2}	5×10^{-2}	10^{-2}	5×10^{-3}	4×10^{-1}
La	4×10^{-4}	2×10^{-3}	5.4×10^{-2}	10^{-2}	10^{-2}	1.7×10^{-1}
Ce	5×10^{-4}	3×10^{-3}	9.8×10^{-2}	10^{-2}	2.1×10^{-2}	2.6×10^{-1}
Sr	1.9×10^{-4}	7×10^{-3}	6.7×10^{-2}	5×10^{-4}	1.1×10^{-3}	1.2×10^{-1}
Nd	10^{-3}	6.8×10^{-3}	2.1×10^{-1}	10^{-2}	8.7×10^{-2}	4.4×10^{-1}
Sm	1.3×10^{-3}	10^{-2}	2.6×10^{-1}	10^{-2}	2.17×10^{-1}	7.6×10^{-1}
Zr	4×10^{-3}	3×10^{-2}	2×10^{-2}	5×10^{-2}	2.5×10^{-1}	5×10^{-1}
Ti	6×10^{-3}	2.4×10^{-2}	10^{-1}	4.8×10^{-2}	10^{-1}	6.9×10^{-1}
Y	4×10^{-4}	9×10^{-2}	7×10^{-1}	10^{-2}	3.8	6×10^{-1}
Yb	1.5×10^{-3}	4.9×10^{-2}	2.8×10^{-1}	10^{-2}	4.03	5.9×10^{-1}

Peridotite modal proportions
(From McKenzie & O'Nions 1992.)

bulk rock	olivine	opx	cpx	gnt/sp/amp
spinel peridotite	0.578	0.270	0.119	0.033
garnet peridotite	0.598	0.211	0.076	0.115
amphibole peridotite	0.599	0.247	0.038	0.116

of F (and hence D) will move downwards with the wedge (figure 2). This analysis neglects the effects of disequilibrium, dispersion and magma mixing before eruption, all of which will tend to reduce the magnitude of the element fractionation and introduce smoother variations in element concentrations with time. However, the simple approach is useful for understanding the relative fractionation of elements by percolation for different fluids and partial melts.

Figure 2 is modified after Davies & Bickle (1991), who developed a physical model

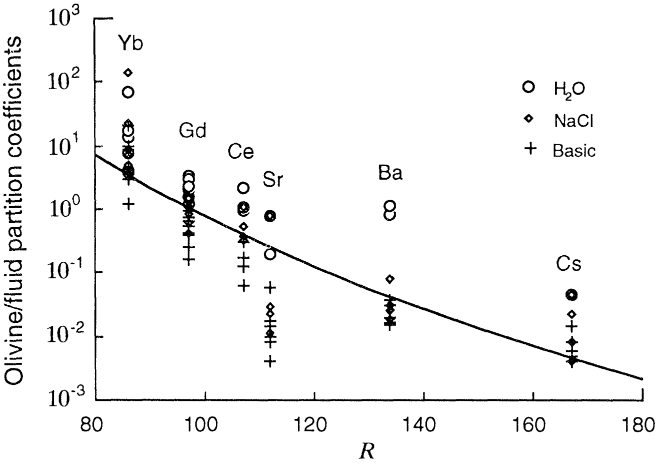

Figure 3. The olivine/fluid partition coefficients for Yb, Gd, Ce, Sr, Ba and Cs measured by Brenan & Watson (1991) plotted against ionic radius (R). The best fit curve is used to estimate partition coefficients for other minor and trace elements with R in the range 69–167 × 10^{-12} m, using values of R from Henderson (1981).

for the volume and composition of melt produced by hydrous fluxing above subduction zones. Hydrous fluids, released into the mantle by dehydration of the subducted slab, traverse the wedge horizontally by a combination of vertical movement as a fluid, and downward movement fixed in amphibole carried down by the induced mantle flow. In such a model, minor and trace elements may be fractionated first by the movement of hydrous fluids, and second of partial melts through the mantle matrix.

Here we wish to evaluate the element fractionation effects of fluid percolation and to do so it is necessary to estimate appropriate partition coefficients. McKenzie & O'Nions (1991) recently compiled mineral/melt partition coefficients for the REEs and some minor elements. These data have been supplemented for other elements and the values used in this work are summarized in table 1. Solid/aqueous fluid partition coefficients are less well known (Eggler 1987), although Brenan & Watson (1991) have recently reported olivine/fluid partition coefficients for several elements and various fluid compositions. Their results indicate that the presence of dissolved salts, in particular carbonates and hydroxides, in the fluid can reduce the partition coefficient relative to pure water by up to two orders of magnitude. Additionally, Tatsumi *et al.* (1986) examined the relative mobility of incompatible elements in hydrous fluids and showed that mobility increases with increasing ionic radius (R), at least in the range for Nb to Cs ($R = 69$ to 167×10^{-12} m). This suggests that there is a relation between R and the solid/fluid partition coefficient, and figure 3 illustrates the olivine/fluid partition coefficients of Brenan & Watson (1991) as a function of ionic radius. As would be expected from the mobility arguments, the partition coefficients decrease with increasing radius, and this relationship has been approximated by a function of the form:

$$Ln(D_{o/f}) = a + b^{*}Ln(R) \tag{3}$$

with $a = 45.63$, $b = -9.97$, and R in $m \times 10^{-12}$. This relationship may be used to predict olivine/fluid partition coefficients for other incompatible elements and, from these and the mineral/melt values mentioned above, and assuming equilibrium

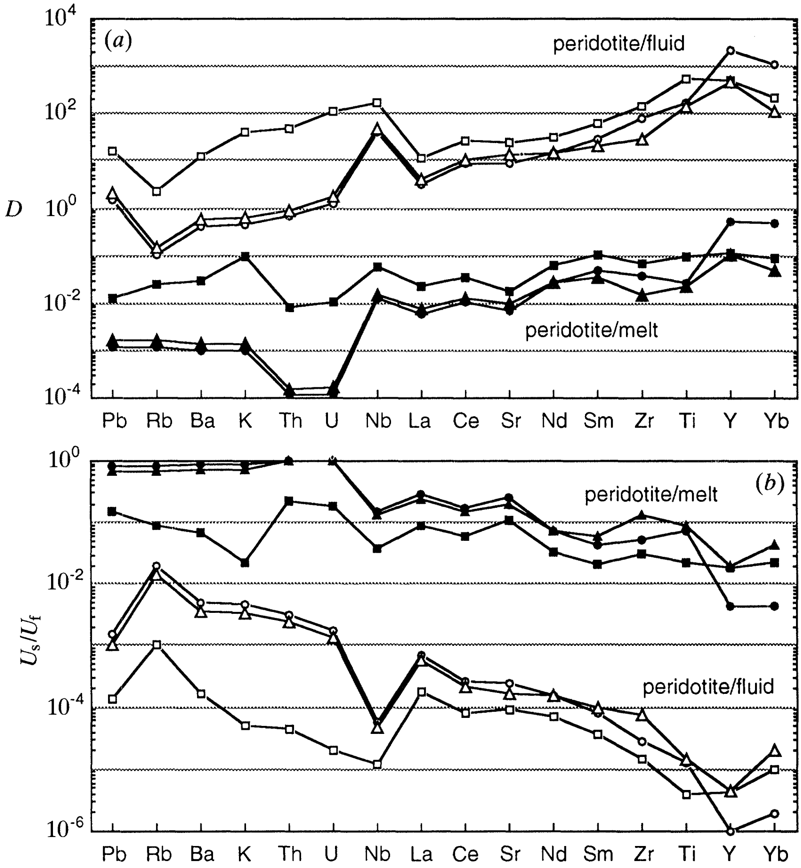

Figure 4. (*a*) Peridotite/fluid partition coefficients calculated from the olivine/fluid partition coefficients of Brenan & Watson (1991), as illustrated in figure 3, compared with the peridotite/melt partition coefficients based on the mineral/melt coefficients in table 1. (*b*) The solid/fluid velocity ratio U_s/U_f, for both melts and hydrous fluids, for which equation (2) with $\alpha = 45°$ is equal to zero. For velocity ratios greater than this critical value elements are expected to be carried down by convection in the wedge, and for lower velocity ratios elements will migrate at some angle above the horizontal (see also figure 2). □, ■, Amphibole peridotite; △, ▲, spinel peridotite; ○, ●, garnet peridotite.

between bulk rock melt and fluid we have estimated bulk rock/fluid partition coefficients according to

$$D_{\mathrm{br/f}} = \frac{D_{\mathrm{o/f}}}{D_{\mathrm{o/m}}} \sum_{j=1}^{N} D_{j\,\mathrm{m}} F_{\mathrm{o}}^{j} = \frac{D_{\mathrm{o/f}}}{D_{\mathrm{o/m}}} D_{\mathrm{br/m}}, \tag{4}$$

where N is the number of mineral phases, $D_{j\,\mathrm{m}}$ and F_{o}^{j} are the mineral/melt partition coefficient and fraction of the jth phase respectively. Figure 4*a* summarizes the calculated bulk rock/melt and bulk rock/fluid partition coefficients for spinel periodotite and amphibole peridotite using the modal proportions from McKenzie & O'Nions (1991). The bulk rock/fluid values are high and this may in part be because all of Brenan & Watson's experimental data were used to constrain $D_{\mathrm{o/f}}$ as a function of R, even though the results for fluids containing dissolved salts alone might be more representative of the real situation. However, the *relative* fractionation between elements should be unaffected by the choice of absolute values for the partition coefficients. We also investigated the correlation between the experimental values of Brenan & Watson (1991) and the ionic charge/radius ratio (Z/R) but could not obtain a significantly better fit to the data. The trends in the calculated partition coefficients using Z/R are broadly similar to those in figure 4*b*, although the range of values is greater, with D_{HFSE} being 2–3 orders of magnitude greater than shown in figure 4*b*, while D_{LILE} being up to a factor of five lower.

Figure 4*b* shows the solid/fluid velocity ratio, U_s/U_f, for both melt and hydrous fluid, for which equation (2), with $\alpha = 45°$, is equal to zero. For velocity ratios greater than this critical value, a given element, travelling with a lower effective velocity than the fluid, will have a sub-horizontal velocity vector, and hence is expected to be carried down by convection in the mantle wedge. At smaller values of U_s/U_f elements will migrate at some angle above the horizontal, and are more likely to arrive at the zone of melt generation. As the dip of the subduction zone decreases, the critical velocity ratio increases, so that more compatible elements may reach the melt generation zone for shallow subduction angles. The velocity ratios for the aqueous fluid are considerably lower than those for melt, because the inferred solid/fluid partition coefficients are much higher. However, as shown by the relevant form of Darcy's law at constant porosity, the velocity of aqueous fluid relative to the matrix is expected to be two or three orders of magnitude higher than that for melt because of the aqueous fluid's lower density and viscosity.

The critical U_s/U_f ratio for different elements largely depends on the differences in their estimated distribution coefficients. Thus for most elements the fluid velocities required for an element to migrate horizontally are significantly greater for amphibole than for spinel peridotite. In detail, it is noticeable that the LILE, and especially U, Th and K, are less enriched relative to the LREEs in the presence of amphibole, and for both peridotites Nb is predicted to be relatively more depleted in the aqueous fluid than in a partial melt.

The implications of such a steady-state equilibrium model for the composition of the source region for arc magmas are that the more fluid compatible elements which are able to move across the flow will tend to maintain their original fluid concentrations which, if adequately enriched, will lead to enrichment of the matrix in the source region. In contrast, the concentration of elements with higher partition coefficients which are carried down with the wedge will be unchanged in the matrix of the source region.

The degree to which the fluid will interact with the matrix and modify its minor and trace element abundances depends on the relative volumes of fluid required to achieve equilibrium with the matrix. To estimate the final source concentration after enrichment we can use limiting values of the original source and fluid concentrations. Thus the mass balance for the source region for the fluid dominated elements is

$$C_s = C_f^0((1-\phi)\,D_{\text{br/f}} + \phi), \tag{5a}$$

where C_f^0 is the initial fluid concentration, $D_{\text{br/f}}$ is the bulk rock/fluid partition coefficient in the wedge and ϕ is the mass fluid fraction present, while the mass balance for the matrix dominated elements in the mantle wedge source region is

$$C_s = C_w^0((1-\phi) + \phi/D_{\text{br/f}}), \tag{5b}$$

where C_w^0 is the initial source or matrix concentration. If the fluid was in equilibrium with the slab then (5*a*) can be expressed in terms of the slab matrix concentration as

$$C_s = (C_{\text{sl}}^0/D_{\text{sl/f}})\,((1-\phi)\,D_{\text{br/f}} + \phi). \tag{5c}$$

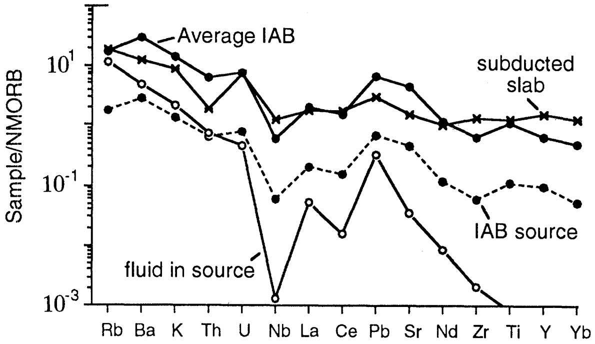

Figure 5. Minor and trace element contents of average island arc basalt; the subducted slab (both from Hawkesworth *et al* 1991*a*); an island arc basalt source calculated assuming for the sake of discussion that average arc basalt is generated by 10% fractional melting of spinel peridotite; and the fluid in equilibrium with that arc basalt source calculated by using the rock/fluid distribution coefficients in figure 4*a*. In the model discussed here, the source for average island arc basalt is developed from a depleted mantle composition (NMORB/10) by interaction with fluid of the composition shown.

The minor and trace element abundances in an arc source were estimated assuming that an average arc basalt (Hawkesworth *et al.* 1991*a*) is the product of 10% fractional melting of spinel peridotite. Using the estimated rock/fluid D values the composition of the fluid in equilibrium with the arc source peridotite was then calculated, assuming 0.5% fluid by volume, although these calculations are not sensitive to the actual value of porosity provided it is small. The results of these calculations are illustrated in figure 5, and although the fluid component is negligible in terms of mass balance within the source region, because $D_{\mathrm{br/f}} > \phi$ and $\phi \ll 1$, the fluid can clearly have a significant effect in terms of modifying the matrix composition, provided local equilibrium is maintained.

To illustrate how a source region may develop over time in the mantle wedge, we can use equation (2) to estimate the minimum velocity required for individual elements to move across the wedge and by specifying a distance to the source region, we can calculate the travel times for each element. For a slab dipping at 45° and a wedge velocity of 30 km Ma^{-1} (Peacock 1991; Davies & Bickle 1991), then the fluid velocity must be greater than 21 km Ma^{-1} for even completely incompatible elements not to be dragged down with the wedge. For a distance of 10 km between the slab and the source region, the maximum travel time for the fluid is 0.47 Ma. However, because of the high D values for the fluid, the fluid velocities need to be much higher than the minimum, implying shorter travel times. In figure 6 we show the travel time as a function of fluid velocity for selected elements for a 10 km distance, U_{s} of 30 km Ma^{-1} and α of 45°. As expected from the relative partition coefficients, the more incompatible elements will be the first to reach the source region for a given fluid velocity. However, the fluid velocities required to enrich even the most incompatible elements are very high. Davies & Bickle (1991) estimated the mass flux of water from the slab to be *ca.* 2×10^5 kg m^{-2} Ma^{-1}, equivalent to an effective velocity of 40 km Ma^{-1} for 0.5% porosity. Although the flux estimates by Peacock (1990) are an order of magnitude higher than that of Davies & Bickle (1991), it is clear that the fluid velocities are unlikely to be as high as the results outlined in figure 6 suggest. The timescales, or velocities, could be reduced if the transport distance is significantly less than the 10 km specified here or, more likely, the estimated

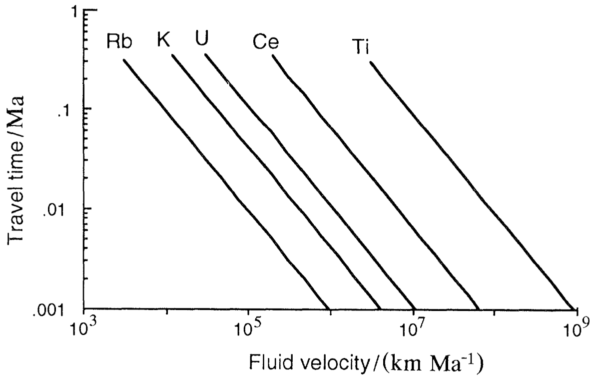

Figure 6. The time taken for the concentration of five elements in the fluid at a point 10 km from the fluid input zone to reach 90 % of the initial fluid values, for a range of fluid velocities. The initial matrix has the minor and trace element content of depleted mantle, and the initial fluid is that calculated to be in equilibrium with the average island arc basalt source in figure 5. If the fluid is in equilibrium with the matrix, the calculated timescales are equivalent to those required for the development of an arc signature in the source peridodite.

partition coefficients are unrealistically large. An order of magnitude reduction in the chosen partition coefficients will result in a broadly similar reduction in element transport times or velocities.

4. Discussion

A model in which the mantle wedge is modified by interaction with a fluid derived from the subducted slab can qualitatively explain many of the distinctive minor and trace element features of destructive plate margin magmas. Such differences between MORB and OIB on the one hand, and IAB on the other, are most readily explained by differences in the partition coefficients into silicate melts and fluids (Pearce 1982) rather than by differences in the residual minerals. Moreover, the available data are consistent with a systematic variation in rock/fluid distribution coefficients and ionic radii, at least in the range $69–167 \times 10^{-12}$ m. Such fluid percolation models account for the key observation that even though island arc rocks are relatively enriched in LILE, the LILE abundances vary less than the HFSE, since it is the LILE which are more likely to reach equilibrium values. However, there are serious problems both in the inferred distribution coefficients outside the range $69–167 \times 10^{-12}$ m and in the high values of the estimated rock/fluid distribution coefficients, which imply unrealistically high fluid velocities (figure 6).

B and Be have very small ionic radii (15×10^{-12} m and 30×10^{-12} m) and so using the extrapolation in figure 3, their inferred olivine/fluid partition coefficients are extremely high (greater than 10^5). However, island arc rocks are characterized by relatively high B/Be and B/LREE ratios, and in some areas by elevated ^{10}Be (Morris *et al.* 1990). Thus it has been argued that B is preferentially mobilized in slab derived fluids, despite its much smaller ionic size than for example the LREE, and that some Be in certain island arc suites is derived from subducted sediment (Morris *et al.* 1990). Moreover, the presence of ^{10}Be in some island arc rocks implies that the transfer time of Be from subducted sediment to the zone of magma generation in the mantle wedge is less than 7.5 Ma (five half-lives of ^{10}Be), and at least for the equilibrium model presented in figure 6 this would require fluid fluxes 3–4 orders of magnitude higher than those suggested by Peacock (1990) and Davies & Bickle (1991). Clearly the distribution coefficients for B and Be extrapolated on the basis of ionic radius are too high, either because in practice their mobility is dramatically increased by the development of complexes (e.g. borates), or rock/fluid D values decrease at low as well as high values of ionic radius and so the curve in figure 3 should not be extrapolated outside the range $69–167 \times 10^{-12}$ m.

In addition to the question of whether the relative partition coefficients for B and Be are too high, it also appears that all the absolute rock/fluid partition coefficients are too high for realistic fluid velocities and time scales (figure 6). In principle radiogenic isotopes can be used as tracers to detect contributions from subducted material in arc rocks, although in practice this signature may be diluted by interaction with the matrix as the fluid moves towards the magma source region (figure 2). Hawkesworth *et. al.* (1991*a*) estimated maximum values for the slab derived contribution in an average arc basalt, assuming no isotope exchange with the mantle wedge. Clearly if exchange occurs such values may be significantly increased. None the less, using their value of 20% for the proportion of Sr derived from the subduced slab, the rock/fluid distribution coefficient would need to be 2–3 orders of magnitude less than that inferred from the Brenan & Watson results, assuming that the transport distance was 10 km and the timescale *ca*. 1 Ma. As discussed by Brenan & Watson (1991) the most likely cause of this discrepancy between the available experimental data and the evidence for element mobility from both high pressure eclogites (Philippot & Selverstone 1991) and mantle xenoliths (Vidal *et al*. 1989), is that the natural systems exhibit more extreme fluid compositions.

Additional constraints on the timescales of trace element transport from the subducted slab to the zone of magma generation are available from U-series disequilibria studies. The majority of subduction-related rocks show relatively little (^{238}U/^{230}Th) disequilibrium, but those that do tend to have high (^{238}U/^{230}Th), and occur in depleted island-arc suites (Gill & Williams 1990; McDermott & Hawkesworth 1991). The presence of excess U requires that U was enriched relative to Th over timescales of less than 350000 years before eruption, and this has been ascribed to U-enriched hydrous fluids derived from the subducted slab (Allègre & Condomines 1982; Condomines *et al*. 1988). If this explanation is correct, and if the disequilibrium is established primarily during slab-dehydration, then for the model discussed here the peridotite/fluid distribution coefficient for U would be not more than 0.001, also three orders of magnitude lower than the value in figure 4*a*. Some of the discrepancy may be because U mobility is sensitive to oxidation state as well as ionic radius, and some may be explained if much of the U excess is established during horizontal fluid transport within the mantle wedge rather than at the slab–wedge interface. None the less the fact that similar discrepancies are inferred for Sr and U reinforces the suggestion that mineral/fluid distribution coefficients must be lower than those used here, presumably because of differences in fluid composition. Additionally, however, we stress that these conclusions are to some extent model dependent in that local equilibrium has been assumed throughout.

Finally, there is the question of partial melting, and how that may vary in different island arcs. It is inferred that partial melting takes place beyond the zone of fluid percolation, as illustrated in figure 2, and several authors have argued that there is little evidence that partial melting beneath arcs results in different element fractionation trends than partial melting elsewhere (Plank & Langmuir 1988). Element ratios such as Ce/Sm may be used as indices of the degree of melting, assuming that some arc magmas are derived from source rocks with similar REE ratios, whereas LIL/HFSE and LIL/REE ratios may reflect fluid fluxes and the amount of water which reaches the magma source regions. The low Ce/Yb arc rocks have similar radiogenic isotope ratios and so they are most likely to have been derived from sources with similar trace element ratios. Furthermore, the systematic variation between average Ce/Sm, but not K/Sm, with crustal thickness in the low Ce/Yb suites (figure 1) suggests that whereas the degree of melting may vary with crustal thickness, this does not appear to be linked in any simple way to differences in the fluid contribution.

Both Plank & Langmuir (1988) and Davies & Bickle (1991) concluded that the degree of partial melting in arcs varies with crustal thickness, and hence with the length of the melting column. However, the inferred amounts of melting varied from 10–25 % to 2–8 % in the two studies, and it was clear that a correlation between the degree of melting and crustal thickness could result from adiabatic decompression and/or be a function of the fact that the mantle is colder in areas of thicker crust. Given that the degree of melting is a nonlinear function of the length of the melting column, and that Ce/Sm varies nonlinearly with degree of melting, the weak correlation between Ce/Sm and crustal thickness in figure 1 may be significant. However, until better data-sets are available we simply conclude that the observed range in Ce/Sm in the low Ce/Yb arcs is consistent with 3–18 % melting of slightly LREE depleted source rocks (see §2), which in the model developed for major elements presented by Davies & Bickle (1991) would suggest that the length of the melting column varies from *ca.* 15 km to over 50 km beneath different arcs.

We thank Huw Davies and Matthew Thirlwall for their thorough and constructive reviews.

References

Allègre, C. J. & Condomines, M. 1982 Basalt genesis and mantle structure studied through Th-isotope geochemistry. *Nature, Lond.* **229**, 21–24.

Arculus, R. J. & Powell, R. 1986 Source component mixing in the regions of arc magma generation. *J. geophys. Res.* **91**, B6, 109–133.

Brenan, J. M. & Watson, E. B. 1991 Partitioning of trace elements between olivine and aqueous fluids at high P–T conditions: implications for the effect of fluid composition on trace element transport. *Earth planet. Sci. Lett.* **107**, 672–688.

Condomines, M., Hemond, Ch. & Allègre, C. J. 1988 U–Th–Ra radioactive disequilibria and magmatic processes. *Earth planet. Sci. Lett.* **90**, 243–262.

Coulon, C. & Thorpe, R. S. 1981 Role of continental crust in petrogenesis of orogenic volcanic associations. *Tectonophys.* **77**, 79–93.

Davies, J. H. & Bickle, M. J. 1991 A physical model for the volume and composition of melt produced by hydrous fluxing above subduction zones. *Phil. Trans. R. Soc. Lond.* A **335**, 355–364.

Eggler, D. H. 1987 Solubility of major and trace elements in mantle metasomatic fluids: experimental constraints. In *Mantle metasomatism* (ed. M. A. Menzies & C. J. Hawkesworth), pp. 21–42. London: Academic Press.

Gill, J. B. & Williams, R. W. 1990 Th isotope and U-series studies of subduction-related volcanic rocks. *Geochim. cosmochim. Acta* **54**, 1427–1442.

Hawkesworth, C. J., Hergt, J. M., Ellam, R. M. & McDermott, F. 1991*a* Element fluxes associated with subduction related magmatism. *Phil. Trans. R. Soc. Lond.* A **335**, 393–405.

Hawkesworth, C. J., Hergt, J. M., McDermott, F. & Ellam, R. M. 1991*b* Destructive margin magmatism and the contributions from the mantle wedge and subducted crust. *Aust. J. Earth Sci.* **38**, 577–594.

Henderson, P. 1982 *Inorganic geochemistry.* (353 pages.) Pergamon Press.

Kay, R. W., Sun, S. S. & Lee-Hu, C. N. 1978 Pb and Sr isotopes in volcanic rocks from Aleutian Islands and Pribilof Islands, Alaska. *Geochim. cosmochim. Acta* **42**, 263–273.

Leeman, W. P. 1983 The influence of crustal structure on compositions of subducted-related magmas. *J. Volcanol. geotherm. Res.* **18**, 561–588.

McDermott, F. & Hawkesworth, C. J. 1991 Th, Pb, and Sr isotope variations in young island arc volcanics and oceanic sediments. *Earth planet. Sci. Lett.* **104**, 1–15.

McKenzie, D. 1984 The generation and compaction of partially molten rock. *J. Petrol.* **25**, 713–765.

McKenzie, D. & O'Nions, R. K. 1991 Partial melt distributions from inversion of rare earth element concentrations. *J. Petrol.* **32**, 1021–1091.

Morris, J. D. & Hart, S. R. 1983 Isotopic and incompatible trace element constraints on the genesis of island arc volcanics from Cold Bay and Amak Island, Aleutians, and implications for mantle structure. *Geochim. cosmochim. Acta* **47**, 2015–2030.

Morris, J. D., Leeman, W. P. & Tera, F. 1990 The subducted component in island arc lavas: constraints from Be isotopes and B–Be systematics. *Nature, Lond.* **344**, 31–36.

Navon, O. & Stolper, E. 1987 Geochemical consequences of melt percolation: the upper mantle as a chromatographic column. *J. Geol.* **95**, 285–307.

Peacock, S. M. 1990 Numerical simulation of metamorphic pressure–temperature–time paths and fluid production in subducting slabs. *Tectonics* **9**, 1197–1211.

Pearce, J. A. 1982 Trace element characteristics of lavas from destructive plate boundaries. In *Andesites: orogenic andesites and related rocks* (ed. R. S. Thorpe), pp. 524–548. New York: Wiley.

Pearce, J. A. 1983 Role of sub-continental lithosphere in magma genesis at active continental margins. In *Continental basalts and mangle xenoliths* (ed. C. J. Hawkesworth & M. J. Norry), pp. 230–249. Nantwich: Shiva.

Philippot, P. & Selverstone, J. E. 1991 Trace-element-rich brines in eclogite veins: implications for fluid composition and transport during subduction. *Contrib. Mineral. Metrol.* **106**, 417–430.

Plank, T. & Langmuir, C. H. 1988 An evaluation of the global variations in the major element chemistry of arc basalts. *Earth planet. Sci. Lett.* **90**, 349–370.

Tatsumi, Y., Hamilton, D. L. & Nesbitt, R. W. 1986 Chemical characteristics of a fluid phase released from a subducted lithosphere and origin of arc magmas: evidence from high pressure experiments and natural rocks. *J. Volcanol. geotherm. Res.* **29**, 293–309.

Tera, F., Brown, L., Morris, J., Sacks, I. S., Klein, J. & Middleton, R. 1986 Sediment incorporation in island-arc magmas: inferences from ^{10}Be. *Geochim. cosmochim. Acta* **50**, 535–550.

Vidal, P., Dupuy, C., Maury, R. & Richard, M. 1989 Mantle metasomatism above subduction zones: trace-element and radiogenic isotope characteristics of peridotite xenoliths from Batan Island (Philippines). *Geology* **17**, 1115–1118.

White, W. M. & Dupré, B. 1986 Sediment subduction and magma genesis in the Lesser Antilles: isotopic and trace element constraints. *J. geophys. Res.* **91**, B6, 5927–5941.

Woodhead, J. D. & Fraser, D. G. 1985 Pb, Sr and ^{10}Be isotopic studies of volcanic rocks from the northern Mariana Island. Implications for magma genesis and crustal recycling in the Western Pacific. *Geochim. cosmochim. Acta* **49**, 1925–1930.